

First-projection-then-regularization hybrid algorithms for large-scale general-form regularization

Yanfei Yang^{a,1,*}

^a*College of Mathematics and Computer Science, Zhejiang A&F University, Hangzhou, 311300, China*

Abstract

The paper presents first-projection-then-regularization hybrid algorithms for large-scale general-form regularization. They are based on a subspace projection method where the matrix A is first projected onto a subspace, typically a Krylov subspace, which is implemented via the Golub-Kahan bidiagonalization process applied to A , with starting vector b . Then we employ a regularization term to the projections. Finally, an iterative algorithm is exploited to solve the resulting inner least squares problems. The resulting algorithms are called *hybrid CGME*(*hyb-CGME*) and *hybrid TCGME*(*hyb-TCGME*). We first prove that the inner least squares problems become better conditioned as k increases, so that the iterative algorithms converge faster. Then we prove how to select the stopping tolerances for *hyb-CGME* and *hyb-TCGME* to solve the resulting inner least squares problems, in order to guarantee that the iterative computed regularized solution and exact computed regularized solutions have the same accuracy. Numerical experiments illustrate that the best regularized solution by *hyb-TCGME* is as accurate as that by *JBDQR* which is a joint bidiagonalization based algorithm, however, the best regularized solution by *hyb-CGME* is a little less accurate than that by *hyb-TCGME* and *JBDQR*. Moreover, from the numerical experiments we can observe that if the rank- k approximation of the projection to A is less accurate, the regularized solution by our hybrid algorithms is also less accurate, at least numerically.

Keywords: First-projection-then-regularization, Hybrid algorithm, General-form regularization, Golub-Kahan bidiagonalization process, CGME, TCGME

2000 MSC: 65F22, 65F10, 65J20, 65F35, 65F50

1. Introduction

Consider the large-scale linear ill-posed problem of the form

$$\min_{x \in \mathbb{R}^n} \|Ax - b\| \quad \text{or} \quad Ax = b, \quad A \in \mathbb{R}^{m \times n}, \quad b \in \mathbb{R}^m, \quad (1)$$

where the norm $\|\cdot\|$ is the 2-norm of a vector or matrix, and A is ill-conditioned with its singular values decaying and centered at zero without a noticeable gap, and the right-hand side $b = b_{true} + e$ is assumed to be contaminated by a Gaussian white noise e , where b_{true} is the noise-free right-hand side and $\|e\| < \|b_{true}\|$. $Ax_{true} = b_{true}$.

Discrete ill-posed problems of the form (1) may be derived from the discretization of linear ill-posed problems, such as the first kind Fredholm integral eqnarray, and arise in various scientific research areas, including biomedical sciences, geoscience and astronomy; see, e.g. [1, 2, 11, 12, 13, 21, 26, 35, 36, 38, 40, 41, 46]. Because of data acquisition noise e and the high ill-conditioning of A , the naive solution $x_{naive} = A^\dagger b$ to (1) generally is meaningless because it bears no relation to the true solution $x_{true} = A^\dagger b_{true}$, where \dagger denotes the Moore-Penrose inverse of a matrix. In order to compute a meaningful solution, it is necessary to employ *regularization* to overcome the inherent instability of ill-posed problems. The basic idea of regularization is that the underlying problem (1) is replaced with

*Corresponding author

Email address: yang@zafu.edu.cn (Yanfei Yang)

¹College of Mathematics and Computer Science, Zhejiang A&F University, Hangzhou, 311300, China

a modified problem which is relatively stable and can obtain a regularized solution to approximate the true solution. There are various regularization techniques taking many forms; see e.g.,[7, 24, 26] for more details.

The simple and popular regularization is by *iterative regularization* to solve the underlying problem (1). In this setting, an iterative method is applied directly to

$$\min_{x \in \mathbb{R}^n} \|Ax - b\|$$

and regularization is obtained by terminating early. It is well known that iterative method exhibits semiconvergence on ill-posed problems, with errors $\|x_k - x_{true}\|/\|x_{true}\|$ decreasing initially but at some point beginning to increase since the small singular values of A start to amplify noise. For iterative regularization, a vital and nontrivial task is to select a good stopping iteration.

Another popular and well established way is general-form regularization, which computes an approximation of x_{true} by solving the following minimization problem

$$\min_{x \in \mathbb{R}^n} \|Lx\| \text{ subject to } \mathbb{S} = \{x \mid \|Ax - b\| \leq \tau\|e\|\} \quad (2)$$

where $\tau \approx 1$ and $L \in \mathbb{R}^{p \times n}$ is a regularization matrix and usually a discrete approximation of some derivative operators. Problem (2) is discrepancy principle based general-form regularization which is equivalent to the following general-form Tikhonov regularization

$$\min_{x \in \mathbb{R}^n} \{\|Ax - b\|^2 + \lambda^2 \|Lx\|^2\}, \quad (3)$$

where $\lambda > 0$ is the regularization parameter that controls the amount of regularization to balance the fitting term and the regularization term; see e.g., [24, 26, 45]. The solution to (3) is unique for a given $\lambda > 0$ when $N(A) \cap N(L) = 0$ where $N(\cdot)$ denotes the null space of a matrix. When $L = I_n$, with I_n being the $n \times n$ identity matrix, problem (2) and problem (3) are said to be in standard form.

The third popular way is the hybrid regularization method. Since O'Leary and Simmons [43] introduce the hybrid methods using Golub-Kahan bidiagonalization and truncated SVD, various hybrid methods based on the Krylov subspace method have been introduced including more general regularization terms and constraints; for more details see, e.g., [5, 6, 7, 8, 9, 14, 15, 16, 18, 27, 39].

Regularization in other norms than the 2-norm are also important. Consider the general optimizations of the form

$$\min_{x \in \mathbb{S}} \mathcal{R}(Lx) \text{ subject to } \mathbb{S} = \{x \mid \mathcal{J}(Ax - b) = \min\}$$

or

$$\min_{x \in \mathbb{R}^n} \{\mathcal{J}(Ax - b) + \lambda^2 \mathcal{R}(Lx)\},$$

where \mathcal{J} is a fit-to-data term and \mathcal{R} is a regularization term. It is known, for instance, that solving

$$\min_{x \in \mathbb{S}} \|Lx\|_p \text{ subject to } \mathbb{S} = \{x \mid \|Ax - b\|_q = \min\} \quad (4)$$

or

$$\min_{x \in \mathbb{R}^n} \{\|Ax - b\|_q + \lambda^2 \|Lx\|_p^p\}, \quad (5)$$

where $1 \leq q < 2$ and $1 \leq p < 2$; see e.g., [15] and [24, pp. 120-121]. Solving problems (4)-(5) need to use nonlinear optimization methods, however, many of these methods require solving a subproblem with an approximate linear model [7, 15, 24].

In this paper, we consider the first-projection-then-regularization hybrid method. The basic idea of the hybrid method is first to exploit a projection method to project the underlying problem onto a relatively stable problem and then employ a regularization term to the projection. Instead of (3), we focus our discussion on problem (2), but the hybrid method we present is fairly general and can be used to solve (4) for a variety of combinations of

fit-to-data term and regularization term. Though, mathematically, (2) is equivalent to (3), numerically, it is totally different between the hybrid method for solving (2) and the one for (3). The former hybrid method has nothing to do with regularization parameter because the number of iteration plays the role of the regularization parameter, and it is the first-projection-then-regularization method. Moreover, the first-projection-then-regularization method for (2) is definitely different from the first-regularization-then-projection one; see [34] for details. The latter hybrid method, however, needs to determine the optimal regularization parameter at every step. Unfortunately, it is difficult to prove the optimal regularization parameter of the projection to be the best regularization parameter of the original problem unless the Krylov subspace captures the singular values in their natural order, starting with the largest, for details see e.g.,[24, 26, 32].

In this paper, we are concerned with the situation when L is fairly general and large. We describe a new projection based hybrid method. First, we use a projection method, where the matrix A is projected onto a increasing subspace, typically a Krylov subspace, and then apply a general-form regularization term to the projection, finally use a iterative algorithm to solve the resulting inner least squares problems. The projection is typically implemented via the Golub-Kahan bidiagonalization process applied to A , with starting vector b . The projections $P_k^T B_k Q_k$ and $P_{k+1}^T C_k Q_{k+1}$ are near best rank- k approximations to A where P_k , P_{k+1} , Q_k and Q_{k+1} are orthogonal columns and B_k is a lower bidiagonalization and C_k is the best rank- k approximation to B_{k+1} . At every step, we use an iterative algorithm to solve the resulting inner least squares problems, which is proved to become better conditioned as k increases, so that the iterative algorithm converges faster. The resulting algorithms are called hyb-CGME and hyb-TCGME, because the projection $P_k^T B_k Q_k$ is based on CGME and another projection $P_{k+1}^T C_k Q_{k+1}$ is based on TCGME. In theory, the inner least squares problems need to be solved accurately. We prove how to choose the stopping tolerance for the iterative algorithm to solve the inner least squares problems, in order to guarantee that the regularized solutions when the inner least squares problems are solved by iterative methods have the same accuracy as the ones when the inner least squares problems are solved exactly. Numerical experiments illustrate that the best regularized solutions by hyb-TCGME are as accurate as the ones by JBDQR in [34], however, the best regularized solutions by hyb-CGME are a little less accurate than the those by hyb-TCGME and JBDQR. Moreover, from the numerical experiments we can observe that if the rank- k approximation of the projection to A is less accurate, the regularized solution by our algorithms is also less accurate, at least numerically.

The organization of this paper is as follows. In Section 2, we briefly review k -step Golub-Kahan bidiagonalization process, CGME and TCGME. We propose the hybrid algorithms and make an analysis on the conditioning of inner least squares problems in Section 3. In Section 4, we make a theoretical analysis on the stopping tolerance for inner least squares problems. Numerical experiments are presented in Section 5. Finally, we conclude the paper in Section 6.

2. k -step Golub-Kahan bidiagonalization process, CGME and TCGME

The lower Lanczos bidiagonalization process is presented by Paige and Saunders [44] which is a variant of the upper bidiagonalization Lanczos process due to Golub and Kahan [19]. Given the initial vectors $\beta_1 p_1 = b$ and $\beta_1 q_0 = 0$, for $i = 1, 2, 3, \dots$, the Golub-Kahan iterative bidiagonalization computes

$$\alpha_i q_i = A^T p_i - \beta_i q_{i-1}, \quad (6)$$

$$\beta_{i+1} p_{i+1} = A q_i - \alpha_i p_i, \quad (7)$$

where $\beta_{i+1} \geq 0$ and $\alpha_{i+1} \geq 0$ are normalization constants chosen so that $\|q_i\| = \|p_{i+1}\| = 1$. In particular, $\beta_1 = \|b\|$.

With the definitions

$$Q_k = (q_1, \dots, q_k), \quad P_k = (p_1, \dots, p_k), \quad (8)$$

and

$$B_k = \begin{pmatrix} \alpha_1 & & & \\ \beta_2 & \alpha_2 & & \\ \dots & \dots & \ddots & \\ & \beta_k & \alpha_k & \end{pmatrix}, \quad B_{k+} = \begin{pmatrix} B_k \\ \beta_{k+1} e_k^T \end{pmatrix}, \quad (9)$$

where e_k is the k -th vector of the standard Euclidean basis vector of \mathbb{R}^k , the recurrence relations (6) and (7) can be written of the form

$$\begin{aligned} A^T P_k &= Q_k B_k^T, \\ A Q_k &= P_{k+1} B_{k+1}. \end{aligned}$$

These matrices can be computed by the following k -step Golub-Kahan bidiagonalization process.

Algorithm 1 k -step Golub-Kahan bidiagonalization process.

1. Take $p_1 = b/\|b\| \in \mathbb{R}^m$, and define $\beta_1 q_0 = 0$.
2. For $j = 1, 2, \dots, k$
 $r = A^T p_j - \beta_j q_{j-1}$
 $\alpha_j = \|r\|$; $q_j = r/\alpha_j$
 $s = A q_j - \alpha_j p_j$
 $\beta_{j+1} = \|s\|$; $p_{j+1} = s/\beta_{j+1}$.

It is well known that CGME [4, 29, 31, 32] is the CG method implicitly applied to

$$\min \|AA^T y - b\| \text{ or } AA^T y = b \text{ and } x = A^T y,$$

and it solves the problems

$$\|x_{\text{naive}} - x_k^{\text{cgme}}\| = \min_{x \in \mathcal{V}_k} \|x_{\text{naive}} - x\|$$

for the iterate x_k^{cgme} , where $\mathcal{V}_k = \mathcal{K}_k(A^T A, A^T b)$ is the k dimensional Krylov subspace generated by the Golub-Kahan bidiagonalization process.

From the k -step Golub-Kahan bidiagonalization process, it follows

$$A = P_k B_k Q_k^T. \quad (10)$$

Noting $\|b\|e_1 = P_k^T b$ and (10), we have

$$x_k^{\text{cgme}} = Q_k B_k^{-1} P_k^T b. \quad (11)$$

Therefore, CGME solves a sequence of problems

$$\min \|P_k B_k Q_k^T x - b\|$$

for x_k^{cgme} starting with $k = 1$, where the projection $P_k B_k Q_k^T$, a rank- k approximation to A , substitutes A in the underlying ill-posed problem (1).

TCGME [32] solves a sequence of problems

$$\min \|P_{k+1} C_k Q_{k+1}^T x - b\| \quad (12)$$

where C_k is the best rank- k approximation for B_{k+1} defined in (9), for x_k^{tcgme} starting with $k = 1$. Obviously, the solution to (12) is

$$x_k^{\text{tcgme}} = Q_{k+1} C_k^{-1} P_{k+1}^T b. \quad (13)$$

About the accuracies of the rank- k approximations $P_k B_k Q_k^T$ and $P_{k+1} C_k Q_{k+1}^T$ to A , Jia has established the following results (cf. [32, Theorem 1 and Theorem 5]).

Theorem 1. For the rank- k approximations $P_k B_k Q_k^T = P_k P_k^T A$ to A , $k = 1, 2, \dots, n-1$, we have

$$\gamma_k^{lsqr} < \gamma_k^{cgme} < \gamma_{k-1}^{lsqr}, \quad (14)$$

$$\gamma_{k+1}^{cgme} < \gamma_k^{cgme}. \quad (15)$$

$$\gamma_k^{tcgme} \leq \theta_{k+1}^{k+1} + \gamma_{k+1}^{cgme} \quad (16)$$

where θ_{k+1}^{k+1} is the smallest singular value of B_{k+1} , $\gamma_k^{cgme} = \|A - P_k B_k Q_k^T\|$, $\gamma_k^{tcgme} = \|A - P_{k+1} C_k Q_{k+1}^T\|$, $\gamma_k^{lsqr} = \|A - P_{k+1} B_{k+1} Q_k^T\|$, and $\gamma_0^{lsqr} = \|A\|$.

Inequalities (14) imply that $P_k B_k Q_k^T$ is definitely a less accurate rank- k approximation to A than $P_{k+1} B_{k+1} Q_k^T$ and there is no guarantee that $P_k B_k Q_k^T$ is a near best rank- k approximation to A even for severely and moderately ill-posed problems; see [32]. It follows from (15) and (16) that

$$\|A - P_{k+1} C_k Q_{k+1}^T\| \leq \theta_{k+1}^{k+1} + \gamma_{k+1}^{cgme} < \theta_{k+1}^{k+1} + \gamma_k^{cgme}.$$

The above relation implies that if θ_{k+1}^{k+1} is very small, then the accuracy of the rank- k approximation $P_{k+1} C_k Q_{k+1}^T$ to A is almost as accurate as $P_{k+1} B_{k+1} Q_k^T$. As there is a lack of theory to guarantee that $P_k B_k Q_k^T$ and $P_{k+1} C_k Q_{k+1}^T$ are the best rank- k approximations to A , which means the solution by CGME or TCGME possibly only has partial regularization [32], we consider to employ regularization term to the projections.

3. The hybrid algorithms: hyb-CGME and hyb-TCGME

Based the above analysis of the accuracies of the rank- k approximations $P_k B_k Q_k^T$ and $P_{k+1} C_k Q_{k+1}^T$ to A , we are interested in a projection based hybrid method for treating large-scale general-form regularization problems with a general matrix L . In the first step, substitute A with $P_k B_k Q_k^T$ or $P_{k+1} C_k Q_{k+1}^T$. The underlying problem is projected onto

$$\|P_k B_k Q_k^T x - b\| = \min \text{ or } \|P_{k+1} C_k Q_{k+1}^T x - b\| = \min. \quad (17)$$

With the iteration, before the semiconvergence, the projection $P_k B_k Q_k^T$ or $P_{k+1} C_k Q_{k+1}^T$ is a near best rank- k approximation to A [32], and then become ill-conditioned, because the matrix B_k usually contains very good approximations to the large singular values of A , it also has singular values which are rough approximations to the small ones [43]. Therefore, in the second step, we consider to employ a regularization term to the projections (17), which means we solve the following problem

$$\min_{x \in \mathbb{S}} \|Lx\| \text{ subject to } \mathbb{S} = \{x \mid \|P_k B_k Q_k^T x - b\| = \min\}, \quad k = 1, 2, \dots, n, \quad (18)$$

or

$$\min_{x \in \mathbb{S}} \|Lx\| \text{ subject to } \mathbb{S} = \{x \mid \|P_{k+1} C_k Q_{k+1}^T x - b\| = \min\}, \quad k = 1, 2, \dots, n. \quad (19)$$

If the projection $P_k B_k Q_k^T$ or $P_{k+1} C_k Q_{k+1}^T$ is the best rank- k approximation to A , then (18) or (19) becomes the MTSVD method [28]. In this sense, the MTSVD method is also a first-projection-then-regularization hybrid method, so is the MTRSVD method [33]. Applying the projection method to (2) can obtain problems (18) and (19). Therefore, (18) and (19) also can be seen as a first-projection-then-regularization hybrid for solving problem (2).

Regarding the hyb-CGME solution $x_{L,k}^{cgme}$ and hyb-TCGME solution $x_{L,k}^{tcgme}$, we can establish the following results.

Theorem 2. Let Q_k and Q_{k+1} be defined in (8). Then the solution to (18) is

$$x_{L,k}^{cgme} = x_k^{cgme} - (L(I_n - Q_k Q_k^T))^\dagger L x_k^{cgme}, \quad (20)$$

and the solution to (19) can be written as

$$x_{L,k}^{tcgme} = x_k^{tcgme} - (L(I_n - Q_{k+1} Q_{k+1}^T))^\dagger L x_k^{tcgme}, \quad (21)$$

where x_k^{cgme} and x_k^{tcgme} are defined in (11) and (13), respectively.

Proof. From Eldén [10], we derive

$$x_{L,k}^{cgme} = (I_n - (L(I_n - (P_k B_k Q_k^T)^\dagger (P_k B_k Q_k^T))^\dagger L)(P_k B_k Q_k^T)^\dagger b$$

and

$$x_{L,k}^{tcgme} = (I_n - (L(I_n - (P_{k+1} C_k Q_{k+1}^T)^\dagger (P_{k+1} C_k Q_{k+1}^T))^\dagger L)(P_{k+1} C_k Q_{k+1}^T)^\dagger b.$$

Combining the above equations with (11) as well as (13), we obtain

$$x_{L,k}^{cgme} = (I_n - (L(I_n - (P_k B_k Q_k^T)^\dagger (P_k B_k Q_k^T))^\dagger L)x_k^{cgme} \quad (22)$$

and

$$x_{L,k}^{tcgme} = (I_n - (L(I_n - (P_{k+1} C_k Q_{k+1}^T)^\dagger (P_{k+1} C_k Q_{k+1}^T))^\dagger L)x_k^{tcgme}. \quad (23)$$

Since B_k is invertible, C_k is the best rank- k approximation to B_k and P_k , P_{k+1} , Q_{k+1} and Q_k are matrices with orthonormal columns, it is straightforward to see that

$$(P_k B_k Q_k^T)^\dagger (P_k B_k Q_k^T) = Q_k Q_k^T \quad (24)$$

and

$$(P_{k+1} C_k Q_{k+1}^T)^\dagger (P_{k+1} C_k Q_{k+1}^T) = Q_{k+1} Q_{k+1}^T. \quad (25)$$

Throwing (24) into (22) yields (20) and, similarly, bringing (25) into (23) derives (21).

From the form of the regularization solutions (20) and (21), these two solutions can be thought of as the iterative solutions (13) and (11) are modified by $(L(I_n - Q_k Q_k^T))^\dagger L x_k^{cgme}$ and $(L(I_n - Q_{k+1} Q_{k+1}^T))^\dagger L x_k^{tcgme}$, respectively. When $L = I_n$, recalling (11) and $Q_k^T Q_k = I_n$, it follows from (20) that

$$\begin{aligned} x_{I,k}^{cgme} &= x_k^{cgme} - ((I_n - Q_k Q_k^T))^\dagger x_k^{cgme} \\ &= (I_n - (I_n - Q_k Q_k^T)) x_k^{cgme} \\ &= Q_k Q_k^T x_k^{cgme} = Q_k Q_k^T Q_k B_k^{-1} P_k^T b \\ &= Q_k B_k^{-1} P_k^T b = x_k^{cgme} \end{aligned}$$

with $((I_n - Q_k Q_k^T))^\dagger = I_n - Q_k Q_k^T$ because $(I_n - Q_k Q_k^T)$ is an orthogonal projection. Similarly, from (13), (21) and $Q_{k+1}^T Q_{k+1} = I_n$, we derive

$$\begin{aligned} x_{I,k}^{tcgme} &= x_k^{tcgme} - ((I_n - Q_{k+1} Q_{k+1}^T))^\dagger x_k^{tcgme} \\ &= (I_n - (I_n - Q_{k+1} Q_{k+1}^T)) x_k^{tcgme} \\ &= x_k^{tcgme} \end{aligned}$$

with $((I_n - Q_{k+1} Q_{k+1}^T))^\dagger = I_n - Q_{k+1} Q_{k+1}^T$ because $(I_n - Q_{k+1} Q_{k+1}^T)$ is an orthogonal projection. This means, when $L = I_n$, the regularized solutions solved by our hybrid algorithms are the ones to standard-form regularization problems.

Let $z_k^{cgme} = (L(I_n - Q_k Q_k^T))^\dagger L x_k^{cgme}$ and $z_k^{tcgme} = (L(I_n - Q_{k+1} Q_{k+1}^T))^\dagger L x_k^{tcgme}$. Therefore, z_k^{cgme} and z_k^{tcgme} are the solutions to the following least squares problems

$$\min_{z \in \mathbb{R}^n} \left\| (L(I_n - Q_k Q_k^T)) z - L x_k^{cgme} \right\| \quad (26)$$

and

$$\min_{z \in \mathbb{R}^n} \left\| (L(I_n - Q_{k+1} Q_{k+1}^T)) z - L x_k^{tcgme} \right\|, \quad (27)$$

respectively, where k is the number of iteration. We now compute the Moore-Penrose inverses of $(L(I_n - Q_k Q_k^T))^\dagger$ in (20) and $(L(I_n - Q_{k+1} Q_{k+1}^T))^\dagger$ in (21) by solving the above two least squares problems.

Evidently, problems (26) and (27) have the same structures. The only difference between them is Q_{k+1} in (27) which has one more column than Q_k in (26). As a consequence, we only show how to solve and analyse (26) in the following.

Due to the large size of $L(I_n - Q_k Q_k^T)$, we suppose that the problems (26) can only be solved by iterative algorithms. We will discuss to use the LSQR algorithm [44] to solve the problems. In order to take fully advantage of the sparsity of L itself and reduce the overhead of computation and the storage memory, it is vital to avoid forming the dense matrix $L(I_n - Q_k Q_k^T)$ explicitly within LSQR. Notice that the only action of $L(I_n - Q_k Q_k^T)$ in LSQR is to form the products of it and its transpose with vectors. We propose Algorithm 2, which efficiently implements the Lanczos bidiagonalization process without forming $L(I_n - Q_k Q_k^T)$ explicitly.

Algorithm 2 \widehat{k} -step Lanczos bidiagonalization process on $L(I_n - Q_k Q_k^T)$.

1. Taking $\beta_1 \widehat{u}_1 = Lx_k$, $\beta_1 = \|Lx_k\|$, $w_1 = L^T \widehat{u}_1$, and define $\widehat{\beta}_1 \widehat{v}_0 = 0$.

2. For $j = 1, 2, \dots, \widehat{k}$

$$\widehat{r} = w_j - Q_k(Q_k^T w_j) - \widehat{\beta}_j \widehat{v}_{j-1}$$

$$\widehat{\alpha}_j = \|\widehat{r}\|; \widehat{v}_j = \widehat{r}/\widehat{\alpha}_j; g_j = Q_k^T \widehat{v}_j$$

$$\widehat{s} = L\widehat{v}_j - L(Q_k g_j) - \widehat{\alpha}_j \widehat{u}_j$$

$$\widehat{\beta}_{j+1} = \|\widehat{s}\|; \widehat{u}_{j+1} = \widehat{s}/\widehat{\beta}_{j+1}; w_{j+1} = L^T \widehat{u}_{j+1}$$

We now consider the solution of (26) using LSQR. Let

$$Q = \begin{pmatrix} Q_k & Q_k^\perp \end{pmatrix} \quad (28)$$

to be an orthogonal matrix and $Q_k^\perp \in \mathbb{R}^{n \times (n-k)}$ to be an orthogonal complement of the matrix Q_k . With the notation of (28), we have

$$L(I_n - Q_k Q_k^T) = LQ_k^\perp (Q_k^\perp)^T \quad (29)$$

and

$$\kappa(L(I_n - Q_k Q_k^T)) = \kappa(LQ_k^\perp (Q_k^\perp)^T) = \kappa(LQ_k^\perp). \quad (30)$$

Relation (30) holds because Q_k^\perp is column orthonormal, the nonzero singular values of $LQ_k^\perp (Q_k^\perp)^T$ are identical to the singular values of LQ_k^\perp .

Next, with the notations, we investigate how the conditioning of (26) changes as k increases.

Theorem 3. *Let the matrix Q_k^\perp be defined in (28) and $L \in \mathbb{R}^{p \times n}$. When $p \geq n - k$, we obtain*

$$\kappa(LQ_k^\perp) \geq \kappa(LQ_{k+1}^\perp), \quad k = 2, 3, \dots, n-1, \quad (31)$$

that is,

$$\kappa(L(I_n - Q_k Q_k^T)) \geq \kappa(L(I_n - Q_{k+1} Q_{k+1}^T)), \quad k = 2, 3, \dots, n-1. \quad (32)$$

Proof. Exploiting the lemma presenting in [20, pp.78] yields

$$\sigma_{\max}(LQ_k^\perp) \geq \sigma_{\max}(LQ_{k+1}^\perp), \quad (33)$$

$$\sigma_{\min}(LQ_k^\perp) \leq \sigma_{\min}(LQ_{k+1}^\perp). \quad (34)$$

From (33), (34) and the definition of the condition of a matrix, we derive

$$\kappa(LQ_k^\perp) = \frac{\sigma_{\max}(LQ_k^\perp)}{\sigma_{\min}(LQ_k^\perp)} \geq \frac{\sigma_{\max}(LQ_{k+1}^\perp)}{\sigma_{\min}(LQ_{k+1}^\perp)} = \kappa(LQ_{k+1}^\perp),$$

which implies (31). Noticing (29), we directly obtain (32) from (31).

Thm 3 indicates that, when applied to solving (26), the LSQR algorithm generally converges faster with k because the worst convergence factor of LSQR is $\frac{\kappa(LQ_k^\perp)^{-1}}{\kappa(LQ_k^\perp)+1}$, see [3, p. 291]. Particularly, in exact arithmetic, LSQR will find the exact solution z_k of (26) after at most $n - k$ iterations.

Exploiting the same method and technology, we can derive the same results for (27) which means we can use Algorithm 2 by replacing Q_k with Q_{k+1} in LSQR to compute z_k^{tcgme} and can attain that the inner iterative algorithm, LSQR with Algorithm 2 to compute (27), is faster convergence with k becoming larger.

Having done the above analysis, now we present the hyb-CGME and hyb-TCGME, named as Algorithm 3 and Algorithm 4, respectively.

Algorithm 3 (hyb-CGME) Given $A \in \mathbb{R}^{m \times n}$ and $L \in \mathbb{R}^{p \times n}$, compute the solution $x_{L,k}^{cgme}$.

- 1: Use Algorithm 1 to compute the projection $P_k^T B_k Q_k$.
- 2: Compute x_k^{cgme} by (11).
- 3: Compute z_k^{cgme} for (26) by LSQR and Algorithm 2.
- 4: Compute the solution $x_{L,k}^{cgme} = x_k^{cgme} - z_k^{cgme}$.

Algorithm 4 (hyb-TCGME) Given $A \in \mathbb{R}^{m \times n}$ and $L \in \mathbb{R}^{p \times n}$, compute the solution $x_{L,k}^{tcgme}$.

- 1: Use Algorithm 1 to compute the projection $P_{k+1}^T C_k Q_{k+1}$.
- 2: Compute x_k^{tcgme} by (13).
- 3: Compute z_k^{tcgme} for (27) by LSQR and Algorithm 2 substituting Q_k with Q_{k+1} .
- 4: Compute the solution $x_{L,k}^{tcgme} = x_k^{tcgme} - z_k^{tcgme}$.

4. The analysis of the stopping tolerance of the inner least squares problems

We highlight that, at step 3 of Algorithm 3-4, we will use the Algorithm 2 to solve the problems with a given tolerance tol as the stopping criterion which substantially exploits the Matlab function `lsqr.m` without explicitly computing the matrix product $L(I_n - Q_k Q_k^T)$ or $L(I_n - Q_{k+1} Q_{k+1}^T)$. We make an insightful analysis and show that the default $tol = 10^{-6}$ is generally good enough and larger tol can be allowed in practical applications. In what follows, for the convenience of writing, we remove the superscript during the analysis, which means we will use z_k instead of z_k^{cgme} and z_k^{tcgme} , x_k instead of x_k^{cgme} and x_k^{tcgme} , and $x_{L,k}$ instead of $x_{L,k}^{cgme}$ and $x_{L,k}^{tcgme}$. Because of using the same algorithm to solve (26) and (27), just like Section 3, we only take (26) as an example.

First of all, with Section 3 notation, we establish the result of the accuracy of the computed solution \bar{z}_k with the stopping tolerance tol in the following lemma.

Lemma 1. *Let z_k and \bar{z}_k be the exact solution and the computed solution by LSQR with the stopping criterion tol to the problem (26), respectively. Then*

$$\frac{\|z_k - \bar{z}_k\|}{\|z_k\|} \leq \frac{\kappa(LQ_k^\perp)}{1 - \eta} \left(2 + \frac{\kappa(LQ_k^\perp) \|r\|}{\|L(I_n - Q_k Q_k^T)\| \|z_k\|} \right) tol, \quad (35)$$

with $r = Lx_k - L(I_n - Q_k Q_k^T)z_k$ and $\eta = tol \cdot \kappa(LQ_k^\perp)$.

Proof. According to [44], the computed solution \bar{z}_k is the exact solution to the perturbed problem

$$\min_{z \in \mathbb{R}^n} \|(L(I_n - Q_k Q_k^T) + E_k)z - Lx_k\|, \quad (36)$$

where

$$E_k = -\frac{r_k r_k^T L(I_n - Q_k Q_k^T)}{\|r_k\|^2}$$

is the perturbation matrix with $r_k = Lx_k - L(I_n - Q_k Q_k^T) \bar{z}_k$ and the stopping tolerance

$$tol = \frac{\|E_k\|}{\|L(I_n - Q_k Q_k^T)\|} = \frac{\|(I_n - Q_k Q_k^T)L^T r_k\|}{\|L(I_n - Q_k Q_k^T)\| \|r_k\|}.$$

Noticing (30) and exploiting the standard perturbation theory [30, p. 382], we obtain

$$\frac{\|z_k - \bar{z}_k\|}{\|z_k\|} \leq \frac{\kappa(LQ_k^\perp)}{1 - \eta} \left(2 + (\kappa(LQ_k^\perp) + 1) \frac{\|r\|}{\|L(I_n - Q_k Q_k^T)\| \|z_k\|} \right) tol. \quad (37)$$

Recalling to the proof of Wedin's Theorem; see [30, pp. 400], we find that the factor $\kappa(LQ_k^\perp) + 1$ in the brace can be replaced by $\kappa(LQ_k^\perp)$ in the context since the right-hand side Lx_k in the perturbed (36) is unperturbed. \square

In applications, L is typically well conditioned [24, 26], so is LQ_k^\perp because of the orthonormality of Q_k^\perp . Therefore, the left hand side of (35) is *at least* as small as $O(tol)$ with a generic constant in $O(\cdot)$.

Define the computed hyb-CGME solution

$$\bar{x}_{L,k} = x_k - \bar{z}_k.$$

We thus have $\|x_{L,k} - \bar{x}_{L,k}\| = \|z_k - \bar{z}_k\|$ by recalling that the hyb-CGME solution

$$x_{L,k} = x_k - z_k.$$

From the above relation and (37) it is reasonable to suppose

$$\frac{\|x_{L,k} - \bar{x}_{L,k}\|}{\|x_{L,k}\|} \leq O(tol) \quad (38)$$

since it is generally impossible that $\|x_{L,k}\|$ is much smaller or larger than $\|z_k\|$.

Let x_L^{opt} be an *optimal* regularized solution to the problem (18) with the white noise e . Then under a certain necessary discrete Picard condition, a GSVD analysis indicates that the error $\|x_L^{opt} - x_{true}\| \geq O(\|e\|)$ with a generic constant in $O(\cdot)$; see [24, p. 83].

Define x_{L,k_0} and \bar{x}_{L,k_0} to be the best regularized solution and the computed best regularized solution by hyb-CGME algorithm, respectively. Obviously,

$$\|x_{L,k_0} - x_{true}\| \geq \|x_L^{opt} - x_{true}\| \geq O(\|e\|). \quad (39)$$

With these notations, the following theorem compares the accurate of the best regularized solution with the computed regularized solution.

Theorem 4. *If L is well conditioned and $\|A\| \approx 1$, then*

$$\frac{\|x_{L,k_0} - x_{true}\|}{\|x_{true}\|} \geq O\left(\frac{\|e\|}{\|b_{true}\|}\right). \quad (40)$$

If

$$O(tol) < \frac{\|e\|}{\|b_{true}\|}, \quad (41)$$

then

$$\left| \frac{\|\bar{x}_{L,k_0} - x_{true}\|}{\|x_{true}\|} - \frac{\|x_{L,k_0} - x_{true}\|}{\|x_{true}\|} \right| \leq O(tol) \quad (42)$$

with a generic constant in $O(\cdot)$.

Proof. Supposing $Ax_{true} = b_{true}$ which means the noise-free problem of (1) is consistent, we have $\|b_{true}\| \leq \|A\|\|x_{true}\|$. Using the inequality, it follows from (39) that

$$\frac{\|x_{L,k_0} - x_{true}\|}{\|x_{true}\|} \approx \|A\| \frac{\|x_{L,k_0} - x_{true}\|}{\|b_{true}\|} \geq \|A\| O\left(\frac{\|e\|}{\|b_{true}\|}\right).$$

Because by suitable scaling $\|A\| \approx 1$ can always be done, we derive (40) from the above relations. Using (37) and (38) as well as $\|x_{L,k_0}\| \approx \|x_{true}\|$ obtains

$$\begin{aligned} \frac{\|\bar{x}_{L,k_0} - x_{true}\|}{\|x_{true}\|} &\leq \frac{\|x_{L,k_0} - x_{true}\|}{\|x_{true}\|} + \frac{\|x_{L,k_0} - \bar{x}_{L,k_0}\|}{\|x_{true}\|} \\ &= \frac{\|x_{L,k_0} - x_{true}\|}{\|x_{true}\|} + \frac{\|x_{L,k_0} - \bar{x}_{L,k_0}\|}{\|x_{L,k_0}\|} \frac{\|x_{L,k_0}\|}{\|x_{true}\|} \\ &= \frac{\|x_{L,k_0} - x_{true}\|}{\|x_{true}\|} + O(tol). \end{aligned} \quad (43)$$

On the other hand, we similarly obtain

$$\frac{\|\bar{x}_{L,k_0} - x_{true}\|}{\|x_{true}\|} \geq \frac{\|x_{L,k_0} - x_{true}\|}{\|x_{true}\|} - O(tol). \quad (44)$$

Combining (43) with (44) obtains

$$\frac{\|x_{L,k_0} - x_{true}\|}{\|x_{true}\|} - O(tol) \leq \frac{\|\bar{x}_{L,k_0} - x_{true}\|}{\|x_{true}\|} \leq \frac{\|x_{L,k_0} - x_{true}\|}{\|x_{true}\|} + O(tol),$$

which implies (42).

Clearly, (40) and (42) imply that, under the condition (41), the computed \bar{x}_{L,k_0} is almost the same as the exact x_{L,k_0} as an approximation to x_{true} . Furthermore, according to the analysis above, we can establish more general results, which include Theorem 4 as a special case.

Theorem 5. *If L is well conditioned and $\|A\| \approx 1$, then*

$$\frac{\|x_{L,k} - x_{true}\|}{\|x_{true}\|} \geq O\left(\frac{\|e\|}{\|b_{true}\|}\right), \quad k = 1, 2, \dots, \min\{m, n\}. \quad (45)$$

Let $\bar{x}_{L,k}$ be the computed solutions obtained by Algorithm 3 using Algorithm 2 with the stopping criterion tol . Then if the condition (41) is satisfied, for $k = 1, 2, \dots, k_0$ and a few $k > k_0$ we have

$$\left| \frac{\|\bar{x}_{L,k} - x_{true}\|}{\|x_{true}\|} - \frac{\|x_{L,k} - x_{true}\|}{\|x_{true}\|} \right| \leq O(tol) \quad (46)$$

with a generic constant in $O(\cdot)$.

Proof. Notice that the x_{L,k_0} is best possible regularized solutions by Algorithm 3 and Algorithm 2 is run for $k = 1, 2, \dots, \min\{m, n\}$, i.e.,

$$\frac{\|x_{L,k_0} - x_{true}\|}{\|x_{true}\|} = \min_{k=1,2,\dots,\min\{m,n\}} \frac{\|x_{L,k} - x_{true}\|}{\|x_{true}\|}. \quad (47)$$

As we all know that, the iterates $\|x_{L,k}\|$ exhibits semiconvergence, which means the iterates $\|x_{L,k}\|$ for $k = 1, 2, \dots, k_0$ tend to be better and better approximations to the exact solution x_{true} , in later stages for $k > k_0$, however, the iterates will start to diverge again from x_{true} and instead converge to the naive solution $x_{naive} = A^\dagger b$. It won't deviate from x_{true} too much for a few $k > k_0$, therefore, for $k = 1, 2, \dots, k_0$ and a few $k > k_0$, we have

$$\frac{\|x_{L,k}\|}{\|x_{true}\|} = O(1). \quad (48)$$

From (47), (48) and the proof of Theorem 4, we attain that when the index k_0 is replaced by $k = 1, 2, \dots, k_0$ and a few $k > k_0$, (40) and (42) also hold under the condition (41). \square

Clearly, (45) and (46) imply that, under the condition (41), the computed $\bar{x}_{L,k}$ is almost the same as the exact $x_{L,k}$ as an approximation to x_{true} for $k = 1, 2, \dots, k_0$ and a few $k > k_0$. It is worthwhile to notice that although the above analysis is for (26), exploiting the same method and technique, for (27) we can get the exactly same results.

What we have to highlight is that the relative noise level $\frac{\|e\|}{\|b_{true}\|}$ is typically more or less around 10^{-3} or 10^{-2} in practice applications, three or four orders bigger than 10^{-6} . From the above analysis, we come to conclude that it is generally enough to set $tol = 10^{-6}$ in LSQR with Algorithm 2 at step 3 of Algorithms 3 and Algorithm 4. A smaller tol will result in more inner iterations without any gain in the accuracy of $\bar{x}_{L,k}$ for $k = 1, 2, \dots, k_0$ and a few $k > k_0$. Moreover, Theorems 4–5 indicate that $tol = 10^{-6}$ is generally well conservative and larger tol can be used, so that LSQR with Algorithm 2 uses fewer iterations to achieve the convergence and the hyb-CGME algorithm and the hyb-TCGME algorithm are more efficient.

To sum up, the conclusion is that a widely varying choice of tol has *no effects* on regularization solution by hyb-CGME and hyb-TCGME, provided that $tol < \frac{\|e\|}{\|b_{true}\|}$ considerably and the regularization matrix L is well conditioned, but it has *substantial effects* on the efficiency of hyb-CGME and hyb-TCGME.

5. Numerical examples

In this section, we report numerical experiments to demonstrate that Algorithm 4 can compute regularized solutions at least as accurately as the JBDQR algorithm in [34] and Algorithm 3 can compute regularized solutions less accurately than JBDQR and Algorithm 4 do. We choose some one dimensional examples from the regularization toolbox [25] and some two dimensional problems from the Matlab Image Processing Toolbox and [2, 42]; see Table 1, where the two dimensional image deblurring problem `mri` is from the Matlab Image Processing Toolbox. We denote the relative noise level

$$\varepsilon = \frac{\|e\|}{\|b_{true}\|}.$$

Table 1: The description of test problems.

Problem	Description	Ill-posedness
<code>shaw</code>	One-dimensional image restoration model [25]	severe
<code>baart</code>	one-dimensional gravity surveying problem [25]	severe
<code>heat</code>	Inverse heat eqnarray [25]	moderate
<code>deriv2</code>	Computation of second derivative [25]	mild
<code>grain</code>	Two dimensional image deblurring [2, 42]	unknown
<code>mri</code>	Two dimensional image deblurring	unknown
<code>satellite</code>	Two dimensional image deblurring [2, 42]	unknown
<code>GaussianBlur440</code>	Two dimensional image deblurring [2, 42]	unknown

Let x^{reg} denote the regularized solution obtained by algorithms. We use the relative error

$$\frac{\|L(x^{reg} - x_{true})\|}{\|Lx_{true}\|}$$

to plot the convergence curve of each algorithm with respect to k . In the tables to be presented, we will list the smallest relative errors and iteration steps in the braces. We use the Matlab function `lsqr.m` and Algorithm 2 avoiding forming the dense matrix $L(I_n - Q_k Q_k^T)$ or $L(I_n - Q_{k+1} Q_{k+1}^T)$ explicitly to compute (26) and (27) with the default stopping tolerance $tol = 10^{-6}$. We have observed that for each test problem, when taking three $tol = 10^{-6}, 10^{-5}$ and 10^{-4} , the computed best regularized solutions by hyb-CGME and hyb-TCGME have the same accuracy. As a consequence, if not explicitly stated, we will only report the results on $tol = 10^{-6}$.

All the computations are carried out in Matlab R2019a 64-bit on 11th Gen Intel(R) Core(TM) i5-1135G7 2.40GHz processor and 16.0 GB RAM with the machine precision $\epsilon_{mach} = 2.22 \times 10^{-16}$ under the Microsoft Windows 10 64-bit system.

5.1. One dimension case

For the four test problems we use the code of [25] to generate A , the true solution x_{true} and noise-free right-hand side b_{true} . They are severely, moderately and mildly ill-posed, respectively. We mention that the problem `deriv2` has three kinds of right-hand sides, distinguished by the parameter "`example` = 1, 2, 3". we only report the results on the parameter "`example` = 2" since we have obtained very similar results on the problem with "`example` = 1, 3". Purely for test purposes, we choose $L = L_1$ defined by

$$L_1 = \begin{pmatrix} 1 & -1 & & & \\ & 1 & -1 & & \\ & & \ddots & \ddots & \\ & & & 1 & -1 \end{pmatrix} \in \mathbb{R}^{(n-1) \times n}. \quad (49)$$

Table 2: The relative errors defined by (35) and the optimal regularization parameters in the braces for the first four test problems in Table 1 with $L = L_1$.

$\varepsilon = 10^{-1}$			
	hyb-CGME	JBDQR	hyb-TCGME
shaw	0.1930(13)	0.1930(13)	0.1732(5)
baart	1.0000(1)	0.6670(1)	0.5509(3)
heat	0.9516(4)	0.3636(1)	0.3689(13)
deriv2	0.8002(2)	1.2761(1)	0.4805(6)
$\varepsilon = 5 \times 10^{-2}$			
	hyb-CGME	JBDQR	hyb-TCGME
shaw	0.9770(3)	1.3390(1)	0.2515(7)
baart	0.9869(2)	0.6063(1)	0.5535(3)
heat	0.7805(5)	0.3470(1)	0.3499(15)
deriv2	0.5907(2)	0.9265(1)	0.4443(9)
$\varepsilon = 10^{-2}$			
	hyb-CGME	JBDQR	hyb-TCGME
shaw	0.9681(4)	0.3237(1)	0.1972(7)
baart	0.8803(3)	0.7054(1)	0.5500(3)
heat	0.5695(9)	0.2146(5)	0.2128(20)
deriv2	0.6113(2)	0.4359(1)	0.6625(3)
$\varepsilon = 10^{-3}$			
	hyb-CGME	JBDQR	hyb-TCGME
shaw	0.3312(6)	0.1246(2)	0.1222(9)
baart	0.5503(3)	0.5257(3)	0.4272(5)
heat	0.3057(15)	0.1427(22)	0.1442(28)
deriv2	0.3826(6)	0.2337(9)	0.5808(2)

In Table 2, we display the relative errors of the best regularized solutions and the optimal regularized parameters by hyb-CGME, JBDQR and hyb-TCGME with $L = L_1$, $m = n = 10,000$ and $\varepsilon = 10^{-1}$, 5×10^{-2} , 10^{-2} , and 10^{-3} , respectively. They illustrate that for all four one dimensional test problems the solution accuracy of hyb-TCGME is every comparable to that of JBDQR and the solution accuracy of hyb-CGME is less accurate than that of JBDQR and hyb-TCGME except shaw and deriv2. For shaw and deriv2, the JBDQR algorithms fails while hyb-CGME and hyb-TCGME works very well, especially hyb-TCGME, which gives the best regularization solutions with high accuracy, when the noises are $\varepsilon = 10^{-1}$ and 5×10^{-2} , respectively. From the table, we observe that hyb-CGME uses less the

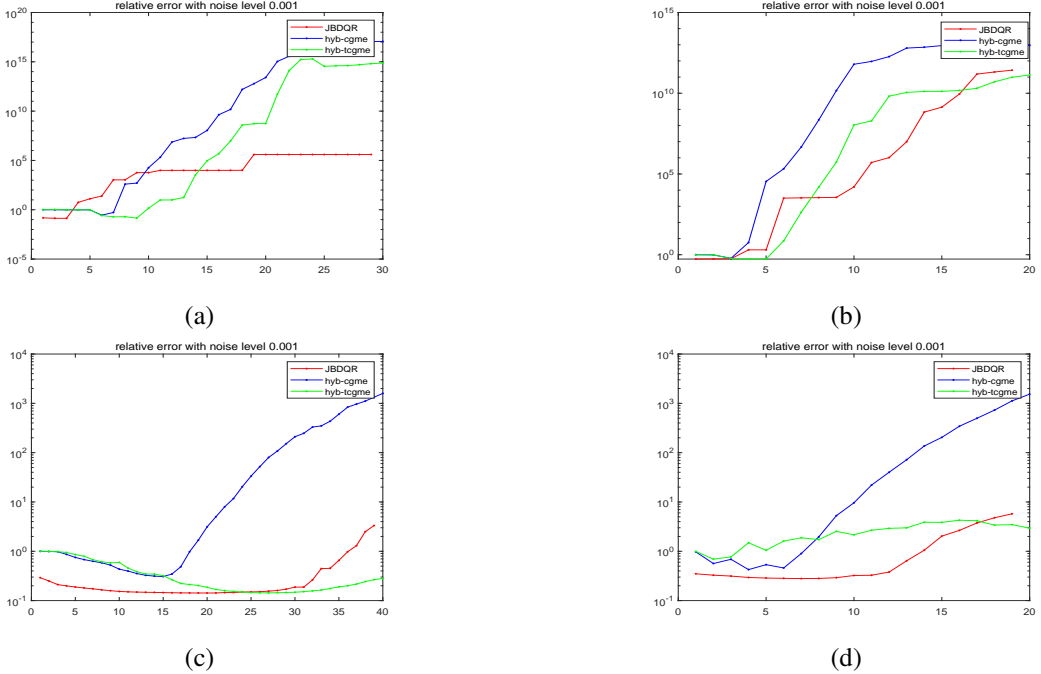


Figure 1: the relative error of hyb-CGME, JBDQR and hyb-TCGME with $L = L_1$ and $\varepsilon = 10^{-3}$ and $m = n = 10,000$: (a) baart; (b) shaw; (c) heat; (d) deriv2.

number of iterations to get a regularized solution than hyb-TCGME and JBDQR do for each test problems. We also observe from the table that for each test problem the lower the noise level of problems is, the more correspondingly accurate of the best regularized solution by each algorithm is; for each algorithm, the lower the noise level of problems is, the bigger the optimal regularization parameter is. All these are expected and justify that the smaller the noise level ε is, the more GSVD dominant components of $\{A, L\}$ are needed to form best regularized solutions.

Figure 1 depicts the convergence processes of hyb-CGME, hyb-TCGME and JBDQR as k increases for the first four test problems with $L = L_1$ and $\varepsilon = 10^{-3}$ and $m = n = 10,000$. We can see that the solution accuracy of the hyb-TCGME algorithm is very comparable to that of the JBDQR algorithm and the solution accuracy of the hyb-CGME algorithm is less accurate than that of JBDQR and hyb-TCGME.

5.2. Two dimension case

In this section, we consider image deblurring problems. The goal in this case is to recover an image x_{true} from a blurred and noisy image $b = b_{true} + e$.

We consider the problems `mri` from the Matlab Image Processing Toolbox. The exact image x_{true} of `mri` is the 15th slice of the three dimensional MRI image dataset which has $N \times N$ pixels. The blurred operator A is a symmetric doubly Toeplitz PSF matrix and is of Kroneck product form $A = (2\pi\sigma^2)^{-1}T \otimes T \in \mathbb{R}^{N^2 \times N^2}$, where $T \in \mathbb{R}^{N \times N}$ is a symmetric banded Toeplitz matrix with half-bandwidth band and σ controls the width of Gaussian PSF. In what follows, $N = 128$, the size of `mri` is $m = n = 128^2 = 16,284$; and $N = 256$, the size of problems `GaussianBlur440`, `grain` and `satellite` is $m = n = 256^2 = 65,536$.

The regularization matrix is chosen as

$$L = \begin{pmatrix} I_N \otimes L_1 \\ L_1 \otimes I_N \end{pmatrix}, \quad (50)$$

where L_1 is defined in (49), which is the scaled discrete approximation of the first derivative operator in the two dimensional case incorporating no assumptions on boundary conditions; see [26, Chapter 8.1-2].

Table 3: The relative errors defined by (35) and the optimal regularization parameters in the braces for the first four test problems in Table 1 with $L = L_1$.

$\varepsilon = 10^{-1}$			
	hyb-CGME	JBDQR	hyb-TCGME
grain	0.9992(4)	0.9524(9)	0.9601(31)
mri	0.9883(2)	0.9134(6)	0.9169(12)
satellite	0.9968(6)	0.9681(13)	0.9682(47)
blur440	0.9913(2)	0.9711(6)	0.9721(21)
$\varepsilon = 5 \times 10^{-2}$			
	hyb-CGME	JBDQR	hyb-TCGME
grain	0.9975(7)	0.9070(19)	0.9237(43)
mri	0.9540(4)	0.8840(12)	0.8873(20)
satellite	0.9924(11)	0.9597(26)	0.9597(61)
blur440	0.9855(4)	0.9654(13)	0.9666(39)
$\varepsilon = 10^{-2}$			
	hyb-CGME	JBDQR	hyb-TCGME
grain	0.9835(22)	0.7089(71)	0.8005(57)
mri	0.8838(12)	0.8412(51)	0.8448(68)
satellite	0.9713(35)	0.9321(132)	0.9345(117)
blur440	0.9717(12)	0.9511(69)	0.9528(159)
$\varepsilon = 10^{-3}$			
	hyb-CGME	JBDQR	hyb-TCGME
grain	0.6486(78)	0.5355(225)	0.5727(148)
mri	0.8262(63)	0.7952(461)	0.8003(459)
satellite	0.9316(84)	0.9002(377)	0.9077(248)
blur440	0.9514(76)	0.9334(622)	0.9349(895)

Table 3 shows the relative errors and the optimal regularization parameters in the braces of algorithms for the test problems with $\varepsilon = 10^{-2}, 5 \times 10^{-2}$ and L defined in (50). We can see that for each test problem the best regularized solution accuracy of JBDQR and hyb-TCGME are very comparable. Meanwhile, we observe that for each test problem the best regularized solution by hyb-CGME is less accurate than the one by JBDQR or hyb-TCGME. From [32] we know that the rank- k approximate to A of the projection by CGME is less accurate than that by TCGME. Therefore, combining Table 2, we observe that if the rank- k approximate to A of the projection is less accurate, the regularized solution is less accurate. This is reasonable, because a good regularized solution must capture the dominant generalized singular value decomposition (GSVD) components of the matrix pair $\{A, L\}$ and meanwhile suppress those corresponding to small generalized singular values; see e.g., [24, 26, 37, 34]. The higher the accuracy of the rank- k approximation of the projection to A , the more likely it is to ensure that hyb-CGME and hyb-TCGME can capture the main generalized singular information of the matrix pair $\{A, L\}$, and the higher the accuracy of the regularized solution by hyb-CGME and hyb-TCGME.

In Figure 2 we display the convergence processes of hyb-CGME, JBDQR and hyb-TCGME for $\varepsilon = 10^{-3}$ and L defined in (50). We can see that the best regularized solutions by hyb-TCGME are almost same as the counterparts by JBDQR except grain and the best regularized solution by hyb-TCGME and JBDQR is better than that by hyb-CGME for the four two dimensional test problems.

The exact images and the reconstructed images for the four two dimensional test problems with $\varepsilon = 10^{-3}$ and L defined in (50) are displayed in Figure 3. Clearly, the reconstructed images by hyb-TCGME are at least as sharp as those by JBDQR and the reconstructed images by hyb-TCGME and JBDQR are much more sharp than the counterparts by

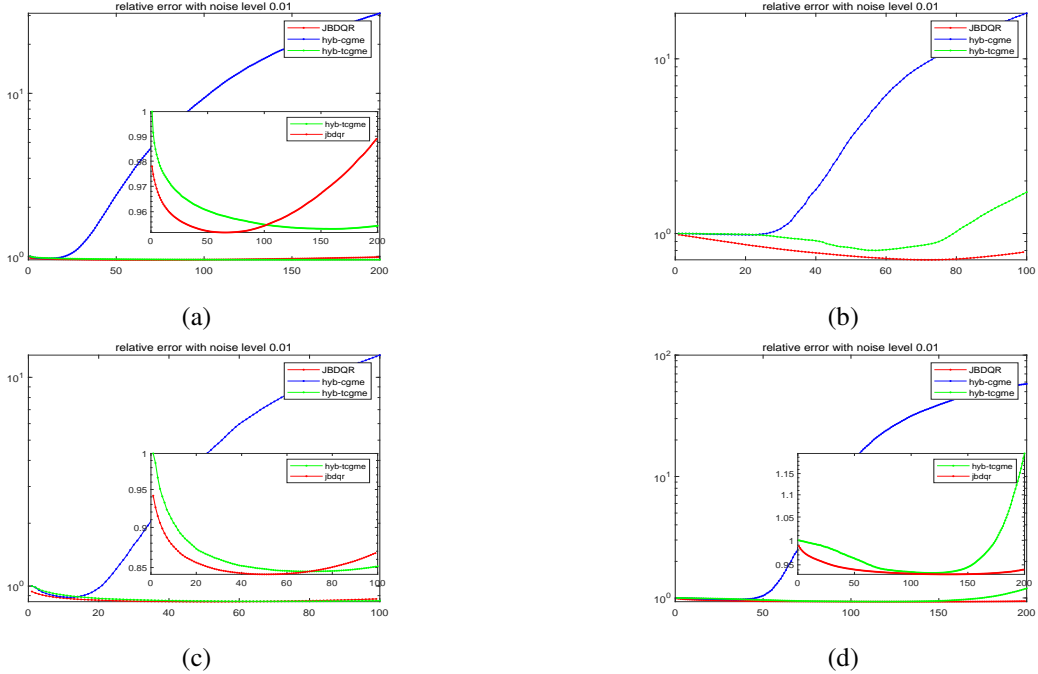


Figure 2: The relative error of hyb-CGME, JBDQR and hyb-TCGME with $\varepsilon = 10^{-2}$ and L defined in (50): (a) blur440; (b) grain; (c) mri; (d) satellite.

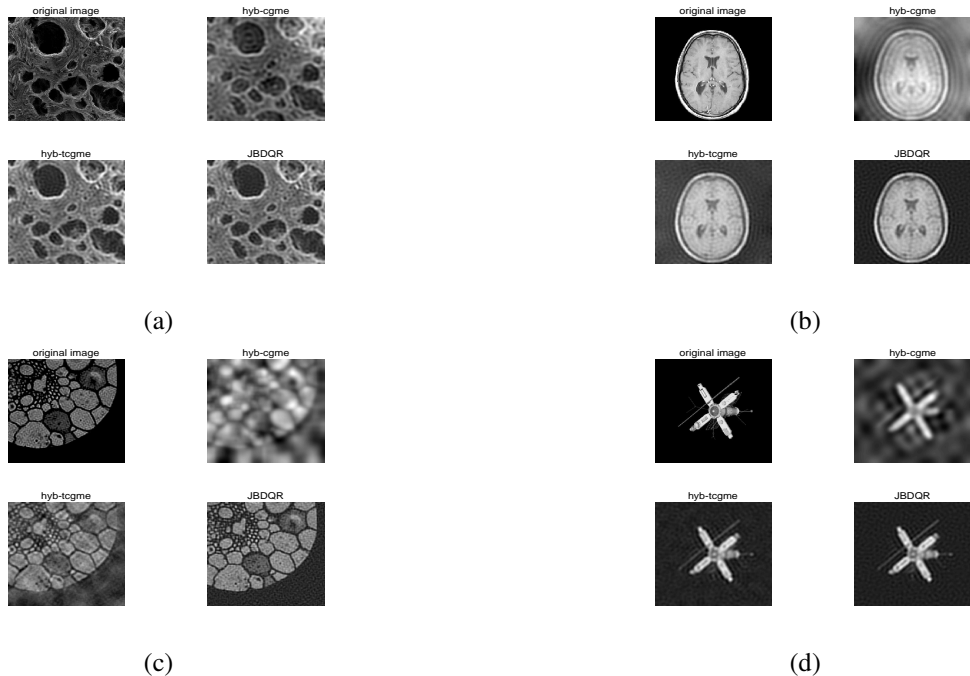


Figure 3: The exact images and the reconstructed images for the four two dimensional test problems with $\varepsilon = 10^{-2}$ and L defined in (50): (a) blur440; (b) mri; (c) grain; (d) satellite.

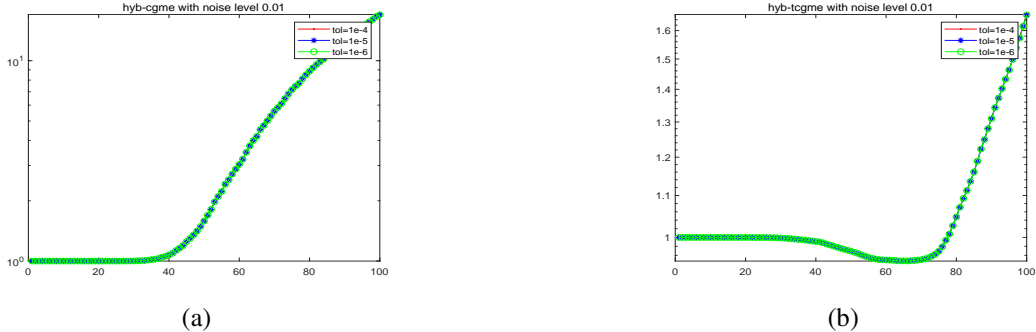


Figure 4: The relative error of grain by hyb-CGME and hyb-TCGME with $\varepsilon = 10^{-2}$ and L defined in (50): (a) hyb-CGME; (b) hyb-TCGME.

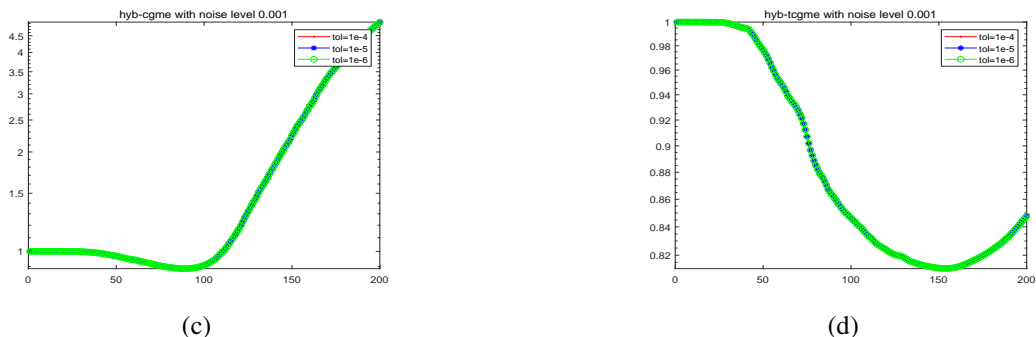


Figure 5: The relative error of grain by hyb-CGME and hyb-TCGME with $\varepsilon = 10^{-3}$ and L defined in (50): (a) hyb-CGME; (b) hyb-TCGME.

hyb-CGME.

In the end, we draw the relative error of grain by hyb-CGME and hyb-TCGME with $\varepsilon = 10^{-2}$ and $\varepsilon = 10^{-3}$ and L defined in (50) in Figure 4 and 5, respectively. Clearly, for grain with $\varepsilon = 10^{-2}$ and $\varepsilon = 10^{-3}$ the computed best regularized solution obtained by hyb-CGME or hyb-TCGME has the same accuracy and the convergence curves of hyb-CGME or hyb-TCGME is indistinguishable when taking three $tol = 10^{-6}, 10^{-5}$ and 10^{-4} . Actually, for each test problem, we have observed the same results. These results confirm Theorems 4-5.

6. Concluding remarks and future work

we have proposed first-projection-then-regularization hybrid algorithms: hyb-CGME and hyb-TCGME for (1) with general-form regularization, which first exploit a subspace projected method, then employ a regularization term to the projections, and finally use Algorithm 2 to solve the resulting inner least squares problems. We have considered the conditioning of inner least squares problems of these two algorithms and shown that it becomes better conditioned as the regularization parameter k increases. As a consequence, Algorithm 2 generally converges faster with k and uses fewer iterations. In the meantime, we have made a detailed analysis on the stopping tolerance of Algorithm 2 for inner least squares problems and shown how to choose it in order to guarantee that the computed regularized solutions have the same accuracy as the ones when the problems are solved exactly. Numerical experiments have confirm our theorem.

Numerical experiments have demonstrated that our hyb-TCGME algorithm can compute regularized solutions with very similar accuracy to the JBDQR algorithm in [34], while our hyb-CGME algorithm can compute regularized solutions which is less accurate than those by hyb-TCGME and hyb-TCGME. Because the rank- k approximation to A by hyb-CGME is less accurate than the one by hyb-TCGME for each test problem and hyb-CGME uses much less iterations to reach the semiconvergence point than hyb-TCGME does for each test problem, hyb-CGME can be chosen to solve the practice applications when these problems don't require high accuracy of the solution but require high efficiency.

There are some important problems that deserve future considerations. The GCV and WGCV methods are $\|e\|$ -free parameter choice methods which can be used when the noise level or the estimation of the noise level is unknown in advance. However, the GCV or WGCV parameter-choice method is not directly applicable to our hyb-CGME and hyb-TCGME algorithm, and some nontrivial effects are needed to derive corresponding GCV or WGCV function. We will consider the GCV and WGCV parameter-choice method for hyb-CGME and hyb-TCGME in future work.

References

- [1] R. C. Aster, B. Borchers and C. H. Thurber, *Parameter Estimation and Inverse Problems*, Second Edition, Elsevier, New York, 2013.
- [2] S. Berisha and J. G. Nagy, *Restore Tools: Iterative methods for image restoration*, available from <http://www.mathcs.emory.edu/~nagy/RestoreTools>, 2012.
- [3] Å. Björck, *Numerical Methods for Least Squares Problems*, SIAM, Philadelphia, PA, 1996.
- [4] Å. Björck, *Numerical Methods in Matrix Computations*, Texts in Applied Mathematics, vol. 59, Springer, 2015.
- [5] F. S. Viloche Bazán, Maria C. C. Cunha and L. S. Borges, Extension of GKB-FP algorithm to large-scale general-form Tikhonov regularization, *Numer. Linear Algebra with Appl.*, 21 (2014), pp. 316–339.
- [6] J. Chung and S. Gazzola, Flexible Krylov methods for l_p regularization, *SIAM J. Sci. Comput.*, 41 (2019), pp. S149–S171.
- [7] J. Chung and S. Gazzola, Computational methods for large-scale inverse problems: A survey on hybrid projection methods, arXiv preprint arXiv:2105.07221, 2021.
- [8] J. Chung and K. Palmer, A hybrid LSMR algorithm for large-scale Tikhonov regularization, *SIAM J. Sci. Comput.*, 37 (2015), pp. S562–S580.
- [9] J. Chung and A. Saibaba, Generalized hybrid iterative methods for large-scale Bayesian inverse problems, *SIAM J. Sci. Comput.*, 39 (2017), pp. S24–S46.
- [10] L. Eldén, A weighted pseudoinverse, generalized singular values and constrained least squares problems, *BIT*, 22 (1982), pp. 487–501.
- [11] H. W. Engl, Regularization methods for the stable solution of inverse problems, *Surveys Math. Indust.*, 3 (1993), pp. 71–143.
- [12] H. W. Engl, M. Hanke and A. Neubauer, *Regularization of Inverse Problems*, Kluwer Academic Publishers, 2000.
- [13] C. L. Epstein, *Introduction to the Mathematics of Medical Imaging*, Second Edition, SIAM, Philadelphia, PA, 2007.
- [14] S. Gazzola and M. S. Landman, Flexible GMRES for total variation regularization, *BIT Numer. Math.*, 59 (2019), pp. 721–746.
- [15] S. Gazzola and J. G. Nagy, Generalized Arnoldi-Tikhonov method for sparse reconstruction, *SIAM J. Sci. Comput.*, 36 (2014), pp. B225–B247.
- [16] S. Gazzola and P. Novati, Automatic parameter setting for Arnoldi-Tikhonov methods, *J. Comput. Appl. Math.*, 256 (2014), pp. 180–195.
- [17] S. Gazzola and P. Novati, Inheritance of the discrete Picard condition in Krylov subspace methods, *BIT Numer. Math.*, 56 (2016), pp. 893–918.
- [18] S. Gazzola, P. Novati and M. R. Russo, On Krylov projection methods and Tikhonov regularization, *Electron. Trans. Numer. Anal.*, 44 (2015), pp. 83–123.
- [19] G. H. Golub and W. Kahan, Calculating the singular values and pseudo-inverse of a matrix, *J. Soc. Indust. Appl. Math. Ser. B Numer. Anal.*, 2 (1965), pp. 205–224.
- [20] G. H. Golub and C. F. Van Loan, *Matrix Computations*, 4th ed., Johns Hopkins Studies in the Mathematical Sciences, Johns Hopkins University Press, Baltimore, MD, 2013.
- [21] E. Haber, *Computational Methods in Geophysical Electromagnetics*, SIAM, Philadelphia, PA, 2014.
- [22] P. C. Hansen, The discrete Picard condition for discrete ill-posed problems, *BIT* 30 (1990), pp. 658–672.
- [23] P. C. Hansen, Truncated singular value decomposition solution to ill-posed numerical rank, *SIAM J. Sci. Comput.*, 11 (1990), pp. 503–518.
- [24] P. C. Hansen, *Rank-Deficient and Discrete Ill-Posed Problems: Numerical Aspects of Linear Inversion*, SIAM, Philadelphia, PA, 1998.
- [25] P. C. Hansen, Regularization tools version 4.0 for matlab 7.3, *Numer. Algor.*, 46 (2007), pp. 189–194.
- [26] P. C. Hansen, *Discrete Inverse Problems: Insight and Algorithms*, SIAM, Philadelphia, PA, 2010.
- [27] P. C. Hansen, Y. Dong and K. Abe, Hybrid enriched bidiagonalization for discrete ill-posed problems, *Numer. Linear Algebra Appl.*, 26 (2019), e2230.
- [28] P. C. Hansen, T. Sekii and H. Shibahashi, The modified truncated SVD method for regularization in general form, *SIAM J. Sci. Comput.*, 13 (1992), pp. 1142–1150.
- [29] M. Hanke, On Lanczos based methods for the regularization of discrete ill-posed problems, *BIT Numer. Math.*, 41 (2001), pp. 1008C1018 Suppl.
- [30] N. J. Higham, *Accuracy and Stability of Numerical Algorithms*, 2nd ed., SIAM, Philadelphia, PA, 2002.
- [31] M. R. Hnětynková, P. Plešinger and Z. Strakoš, The regularizing effect of the Golub-Kahan iterative bidiagonalization and revealing the noise level in the data, *BIT Numer. Math.*, 49 (2009), pp. 669–696.
- [32] Z. Jia, Regularization properties of Krylov iterative solvers CGME and LSMR for linear discrete ill-posed problems with an application to truncated randomized SVDs, *Numer. Algor.*, 85 (2020), pp. 1281–1310.
- [33] Z. Jia and Y. Yang, Modified truncated randomized singular value decomposition (MTRSVD) algorithms for large scale discrete ill-posed problems with general-form regularization, *Inverse Probl.*, 34 (2018), 055013.
- [34] Z. Jia and Y. Yang, A joint bidiagonalization based algorithm for solving large-scale ill-posed problems in general-form regularization, *Appl. Numer. Math.*, 157 (2020), pp. 159–177.
- [35] J. Kaipio and E. Somersalo, *Statistical and Computational Inverse Problems*, Springer, Science & Business Media, 2006.
- [36] M. Kern, *Numerical Methods for Inverse Problems*, Wiley, 2016.
- [37] M. E. Kilmer, P. C. Hansen and M. I. Españo, A projection-based approach to general-form Tikhonov regularization, *SIAM J. Sci. Comput.*, 29 (2007), pp. 315–330.

- [38] A. Kirsch, An Introduction to the Mathematical Theory of Inverse Problems, 2nd edn. Springer, New York, 2011.
- [39] J. Lampe, L. Reichel and H. Voss, Large-scale Tikhonov regularization via reduction by orthogonal projection, *Linear Algebra Appl.*, 436 (2012), pp. 2845–2865.
- [40] K. Miller, Least squares methods for ill-posed problems with a prescribed bound, *SIAM J. Math. Anal.*, 1 (1970), pp. 52–74.
- [41] F. Natterer, The Mathematics of Computerized Tomography, SIAM, Philadelphia, 2001.
- [42] J. G. Nagy, K. Palmer, and L. Perrone, Iterative methods for image deblurring: A Matlab object-oriented approach, *Numer. Algor.*, 36 (2004), pp. 73–93
- [43] D. O’Leary and J. Simmons, A bidiagonalization-regularization procedure for large scale discretizations of ill-posed problems, *SIAM J. Sci. Stat. Comput.*, 2 (1981), pp. 474–489.
- [44] C. C. Paige and M. A. Saunders, LSQR: An algorithm for sparse linear equations and sparse least squares, *ACM transactions on mathematical software* 8 (1982), pp. 43–71.
- [45] A. N. Tikhonov, Solution of incorrectly formulated problems and the regularization method, *Soviet Math.*, 4 (1963), pp. 1035–1038.
- [46] C. R. Vogel, Computational Methods for Inverse Problems,